1 Supplemental Material

1.1 Data evaluation

Determination of the measured pressure

The wall movement in the midplane of the channel ($z = 0.5h$) was determined by tracking the tracer particles embedded in the PDMS with the custom made software OpenBox[1]. Approximately 80 beads within the first 30 μm to the wall were tracked and averaged over 3 oscillation periods on each side of the channel to obtain the lateral motion $Y_{\text{left}}, Y_{\text{right}}$ on each side of the channel. The strain ε of the PDMS is related to the periodic wall movement $Y(x,t) = 0.5(Y_{\text{left}} - Y_{\text{right}}) - Y_0(p = 0)$ via a geometrical factor $\varepsilon = f_{\text{geom}}Y/w$, where w is the lateral channel width. f_{geom} was determined in a FEM-simulation (Multiphysics, COMSOL) for a channel (w x $h = 60$ x $80\,\mu\text{m}^2$) with a 1000 x 1000 x 80 μm^3 inlet section and has a constant value of $f_{\text{geom}} \approx 0.95$ except within the first 1 mm next to the channel entrance and exit (see Fig. 5b).

The pressure for each Fourier component of the strain $\varepsilon(x,t) = \sum_{n=0}^{\infty} \varepsilon_n(x)\exp\left[i(\omega_n t + \varphi_n)\right]$ can now be calculated with the complex shear modulus $G^*(\omega)$ using the Poisson ratio of 0.5 for PDMS

$$p_n(x,t) = 3|G^*(\omega_n)| \cdot \varepsilon_n \exp[i(\omega_n t + \varphi_n - \delta(\omega_n))] \tag{S1}$$

where $\tan\delta(\omega) = G''(\omega)/G'(\omega)$ and $\omega_n \equiv n\omega_0$. $G^*(\omega)$ was measured with an AR-G2 (TA-Instruments, Delaware) oscillatory rheometer with a 2° cone-plate geometry for a constant strain $\varepsilon = 0.1\%$ (see Fig. 6). The pressure pulse can then be computed directly from the wall movement $Y(x,t) = \sum_{n=0}^{\infty} Y_n \exp\left[i(\omega_n t + \varphi_n)\right]$ with:

$$p(x,t) = \sum_{n=0}^{\infty} 3|G^*(\omega_n)|\frac{f_{\text{geom}}}{w}Y_n(x,t)e^{i(\omega_n t + \varphi_n - \delta(\omega_n))} \tag{S2}$$

Computation of the flowrate

A self-written Particle Image Velocimetry (PIV) algorithm was used to extract the flowrate. The channel region of the videos was divided into 11 stripes which were correlated frame by frame, and three oscillation periods were averaged to yield the velocity $v(x,t)$ in one period. A parabolic fit over the obtained flow profile was used to extract the maximum velocity $v_{max}(x,t)$ in the middle of the channel for each frame. The flowrates Q were then calculated from v_{max} for $w < h^2$:

$$\frac{v_{\text{max}}}{Q} = \frac{48}{\pi^3 hw}\frac{\sum_{n,\text{odd}}^{\infty} \frac{(-1)^{\frac{n-1}{2}}}{n^3}\left[1 - \frac{1}{\cosh(n\pi\frac{h}{2w})}\right]}{1 - 0.63\frac{w}{h}} \tag{S3}$$

The flowrate curves Q differ less than 5 % from their steady state values $Q_{s.s.}$ at the end of half the period of the driving oscillation $T_0/2 = \pi/\omega_0 = 1$s. The steady state flowrate has to be equal at all channel positions — yet the measured steady state maximum velocities vary up to 20 %, possibly due to local inhomogeneities in the channel geometry and variations in the z-position. To account for these sources of uncertainty the absolut values of the velocity curves were scaled to yield matching steady state flowrates $Q_{s.s.}$ for the different channel positions (shown in Fig. 3b), which does not alter the shape of the flowrate pulses and the frequency dependencies discussed.
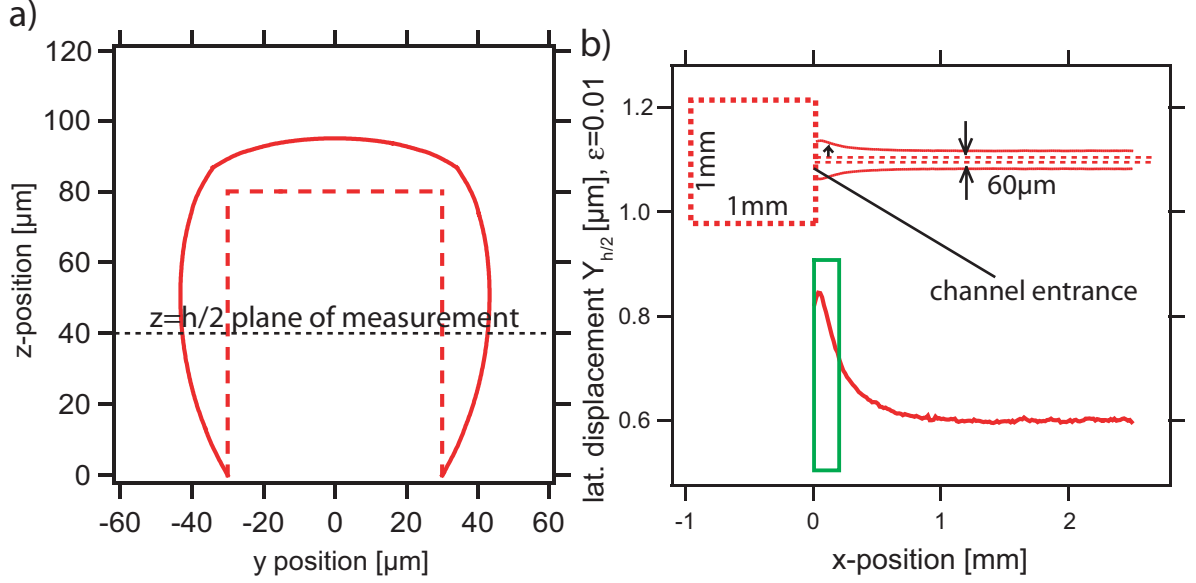
Figure 5: FEM-simulations to determine f_{geom} and k_{geom}. (a) Channel expansion corresponding to $\varepsilon = 0.01$ in cross-section of PDMS channel. For clarity the wall displacement has been 20x enlarged. (b) Wall displacement $Y(z = h/2)$ along the channel. Near the channel entrance at $x = 0$ the expansion of the channel is higher than inside the channel. The green box shows the area recorded in the video for $Y(x = 0), Q(x = 0)$.

1.2 Calculation of theoretical curves

All theoretical curves were computed using the measured pressure at $x = 0$. Solving eq. (2) for $x = 7.5, 12.5$ and 17.5 mm gives theoretical curves for p and Q along the channel. The parameters $Z_x(\omega)$ and R_x were determined as described in the following.

Determination of $Z_x(\omega)$:

The complex susceptibility of the PDMS walls $Z_x(\omega) = \frac{1}{g_x} + \frac{1}{i\omega C_x}$ was determined from adapting a Maxwell body. The hydrodynamic capacitance of the channel $C_x(\omega)$ is proportional to the strain, the channel cross-section and a geometric factor k_{geom}:
$C_x(\omega) = \frac{k_{\text{geom}} wh\varepsilon}{p_n(1+i\tan\alpha)}$

The phase difference of α between p and ε is adjusted to the measured phasedifference $\tan\delta = \tan\alpha = \omega C_x/g_x$ and eq. (S2) gives for each Fourier-component p_n:

$$|p_n| = \frac{k_{\text{geom}} wh\varepsilon_n}{C_x \cos\delta} = 3|G^*|\varepsilon \qquad (S4)$$

i.e. $C_x(\omega_n) = \frac{C_{x,0}}{|G^*(\omega_n)/G^*_{\omega_0}|\cos\delta}$ and $g_x = \frac{\omega_n C_{x,0}}{|G^*(\omega_n)/G^*_{\omega_0}|\sin\delta}$ with $C_{x,0} = \frac{k_{\text{geom}} wh}{3|G^*_{\omega_0}|}$. The FEM-simulation (Fig. 5a) suggests a geometrical factor $k_{\text{geom}} = 2.4$. The best accordance with the experimental data was achieved with $k_{\text{geom}} = 2.0$, which has been used for the theoretical calculations.

Determination of hydrodynamic resistance R_x:

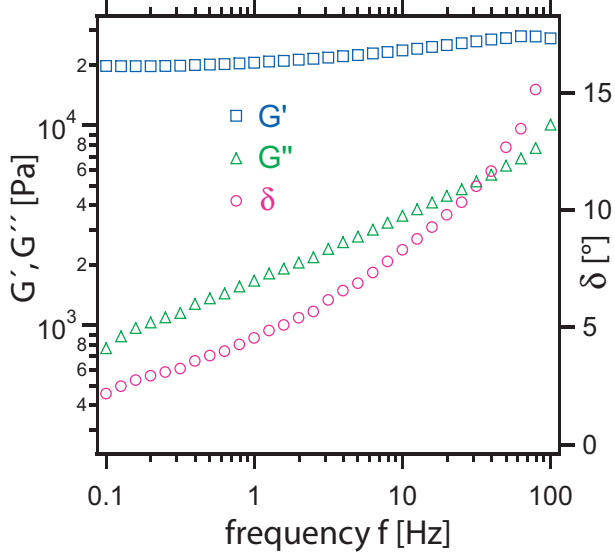The hydrodynamic resistance per unit length R_x for a rectangular channel filled

2

Figure 6: Oscillatory rheometer measurement of the complex shear modulus $G^* = G' + iG''$ of PDMS with phase angle δ between stress and strain.

with fluid of viscosity η for $w < h$ is given by [2]:

$$R_x \approx \frac{12\eta}{w^3 h}\left(1 - 0.63\frac{w}{h}\right)^{-1}.$$ (S5)

The changes of the channel cross-section due to the applied pressure in the experiment are small ($< 3\%$), thus the resistance can be assumed to be independent of the applied pressure $R_x = const$. Especially in shallow channels and at higher operating pressures the dependence of the hydrodynamic resistance $R_x(p(x))$ on the pressure can be quite significant and has to be considered [3,4].

Determination of hydrodynamic inductance L_x:

The hydrodynamic inductance per unit length L_x for a circular tube with cross-sectional area A is given as $L_x = \rho/A$ where ρ is the fluid density [5]. For the theoretical curves $L_x = \rho/A$ was used for the rectangular channel with $A = wh$ using a fluid density of $\rho = 1.2\,\text{gcm}^{-3}$.

Determination of fluid viscosity η:

A consistent value for the viscosity η can be extracted from the periodic measurement in the channel itself: Since $\omega_0 < \omega_{\text{cutoff}}$, p and Q at the end of the period of the step pulses are good estimates for the steady state values $p_{s.s.}$ and $Q_{s.s.}$ in constant flow. The overall resistance of the channel $R_x l$ has to fulfill the equation $R_x l = \frac{p_{s.s.}}{Q_{s.s.}}$ which directly sets an experimental value for the viscosity of

$$\eta = \frac{p_{s.s.}}{Q_{s.s.}l}\frac{h^3 w}{12}\left(1 - 0.63\frac{h}{w}\right)$$ (S6)

Calculation of phase velocity $v_{ph}(\omega_n)$:

To calculate the phase velocity of the pressure propagation we evaluate the phase difference $\Delta\Phi_{0-x_i}^{n,p}$ of the Fourier component of the pressure $p_n(\omega_n)$ between the channel entrance $x = 0$ and position $x = x_i$. From there we can determine the apparent phase

velocity $v_{ph}(\omega_n)$ with which a point with a given phase of p_n travels along the channel [6]:

$$v_{ph}(\omega_n, x_i) = -\omega_n / \left(\frac{\mathrm{d}(\Delta\Phi_{0-x_i}^{n,p})}{\mathrm{d}x_i} \right) \tag{S7}$$

To enable a comparison with the experimental data, we define an average phase velocity $\overline{v}_{ph}(\omega_n)$ for the propagation from the channel entrance $x = 0$ to $x = x_i$ by replacing $\mathrm{d}(\Delta\Phi_{0-x_i}^{n,p})/\mathrm{d}x_i$ with the phase difference and the traveled distance $\Delta x = x_i$: $\overline{v}_{ph}(\omega_n, x_i) = -x_i\omega_n/\Delta\Phi_{0-x_i}^{n,p}$. In the low frequency limit $\omega \ll \omega_{\mathrm{cutoff}}$ the viscous dissipation of the PDMS channel wall is negligible ($\delta \approx 0$) and we obtain a phase velocity of $v_{ph}(x_i) = \frac{3D_p}{l-x_i}$ and an average phase velocity $\overline{v}_{ph}(\omega_n)(0 \to x_i)$: $\overline{v}_{ph}(x_i) = \frac{6D_p}{2l-x_i}$ which are independent of the frequency but dependent on the x-position along the channel.

For high frequencies $\omega \gg \omega_{\mathrm{cutoff}}$ with $\delta \approx 0$ we get a phase velocity of

$$v_{ph}(\omega_n) = \overline{v}_{ph}(\omega_n) = \sqrt{\frac{2\omega_n D_p}{\cos\delta(1-\sin\delta)}}$$

which is independent of x_i and thus equal to the averaged phase velocity.

References

[1] J. Schilling, E. Sackmann and A. Bausch, *Rev Sci Instrum*, 2004, **75**, 2822–2827.

[2] H. Bruus, *Theoretical Microfluidics*, Oxford University Press, 2007.

[3] T. Gervais, J. El-Ali, A. Günther and K. Jensen, *Lab on a Chip*, 2006, **6**, 500–507.

[4] B. Hardy, K. Uechi, J. Zhen and H. Kavehpour, *Lab on a Chip*, 2009, **7**, 935–938.

[5] W. Nichols, *McDonald's Blood Flow in Arteries* , Oxford University Press, 2005.

[6] M. Taylor, *Physics in Medicine and Biology*, 1957, **1**, 321–329.